Analyst

Accepted Manuscript

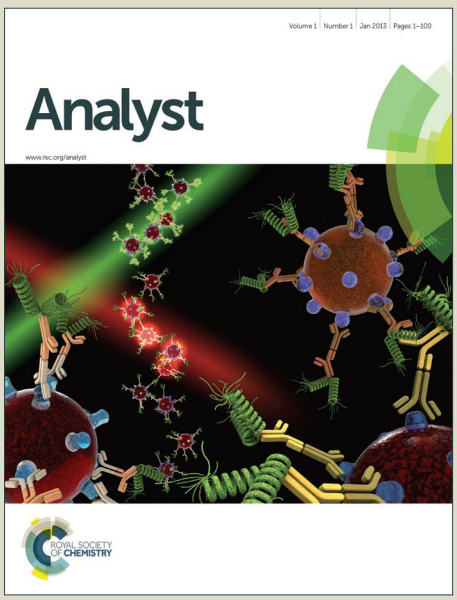

ROYAL SOCIETY OF CHEMISTRY

www.rsc.org/analyst

Analyst

ARTICLE

Ratiometric fluorescent sensor array based on quantum dots for detection of proteins

Received 00th January 20xx,
Accepted 00th January 20xx

DOI: 10.1039/x0xx00000x

www.rsc.org/

Ning Chang,[a] Yuexiang Lu,[b] Jinpeng Mao,[a] Jiaoe Yang,[a] Mengnan Li,[a] Sichun Zhang,[c] Yueying Liu,*[a]

Optical cross-reactive sensor arrays have recently been demonstrated as a powerful tool for high-throughput protein analysis. Nevertheless, applying this technology to the protein detection is complicated by many external factors, such as the interfering substances, the background noise, and sample environmental changes in biological matrix. Herein we demonstrated that the ratiometric fluorescence sensor array based on quantum dots can be employed to circumvent these limitations. Several intrinsic dual-emitting Mn-doped quantum dots capped by different organic functional groups were designed as sensing elements. Distinct and reproducible response patterns against the ratiometric sensor array were obtained from ten proteins in the buffer of different pH (pH 5.7, 7.4, and 8.3) and spiked into human urine. Linear discrimination analysis of the response patterns showed successful differentiation of the analytes at concentrations as low as 50 nM with high identification accuracy. Furthermore, this sensor system also enables these eight proteins (at 500 nM) within human urine without any treatment. The ratiometric fluorescence change from quantum dots for analysis of proteins can eliminate effectively the signal interference from pH value change and fluorescent background in human urine. The present study will open a new avenue to improve discrimination ability of sensor array.

Introduction

Optical cross-reactive sensor arrays often termed 'chemical noses/tongues' have recently been demonstrated as a powerful tool for high-throughput targets analytes (protein, cell, tissue, bacteria, and so on) detection.[1] There are two key strategies for improving the sensitivity and discrimination ability: to add the number of sensing acceptors and extract more than one signal from a single sensing material. Notably, semiconductor quantum dots (QDs) have been used for the configuration of various fluorescence sensor arrays due to high fluorescence efficiency, narrow and symmetric emission with tunable colors, broad absorption, and versatile surface modification.[2] The cancer cell type and phenotype were successfully differentiated using the sensor array based on the conjugates of quantum dots and gold nanoparticles.[3] Four QDs nanoprobes with different ligand receptors were successfully used to identify different nucleobases.[4] These fluorescent sensor arrays are only involved in a singular response of fluorescence quenching or brightening. It is obvious that the sensitivity and discrimination ability of these array are critically dependent on the number of sensing elements. On the other hand, QDs also have been employed to give multidimensional sensory information for discrimination of proteins. Particularly, doping the QDs with trace impurities enables an alteration or an increase of the number of emission centers.[5] Mn-doped ZnS (Mn-ZnS) QDs are the most studied doped QDs, which show unique and well-resolved dual emission bands under a single wavelength excitation, respectively.[6] A phosphorescent (Ph) and resonant light scattering (RLS) dual-channel sensing system based on protein-coated Mn-ZnS QDs was developed for biosensing of trypsin and lysozyme.[7] Besides the two channels of Ph and LS signals used for the Mn-ZnS-QDs-based sensor arrays, the fluorescence polarization (FP) was added as a signal channel for further improving the capability of sensor array based on the phenylboronic acid derivatives QDs to discriminate glycoproteins.[8] A multidimensional sensing device based on simultaneous utilization of the triple-channel optical properties (FL, Ph, LS) of Mn-ZnS QDs was reported on the discrimination of proteins.[9] It is evident that increasing the dimensionality of sensor array can improve the discrimination and quantification of target analytes. Nevertheless, in some cases, extracting more information of sensor may even lower the performance of the array, because the added information could be irrelevant to the discrimination and quantification of target compounds. Even worse, the feature is sensitive to the interfering substances or the chemical background,[10] the sensitivity and discrimination ability of multidimensional sensor is lower. Obviously, the signal response changes of these two different transduction principles are gained from correlated optical properties of QDs, which could be not perfectly orthogonality or complementary information. Therefore, the discrimination ability of sensor array is restricted by multidimensional information based on QDs in a lab-on-a-molecule approach.

[a]*Department of Chemistry, Capital Normal University, Xisanhuan North Rd. 105, Beijing, 100048, P.R. China*
[b]*Institute of Nuclear and New Energy Technology, Tsinghua University, Beijing 100084, P.R. China*
[c]*Department of Chemistry, Tsinghua University, Beijing, 100084, P.R. China*
†Electronic Supplementary Information (ESI) available: [details of any supplementary information available should be included here]. See DOI: 10.1039/x0xx00000x

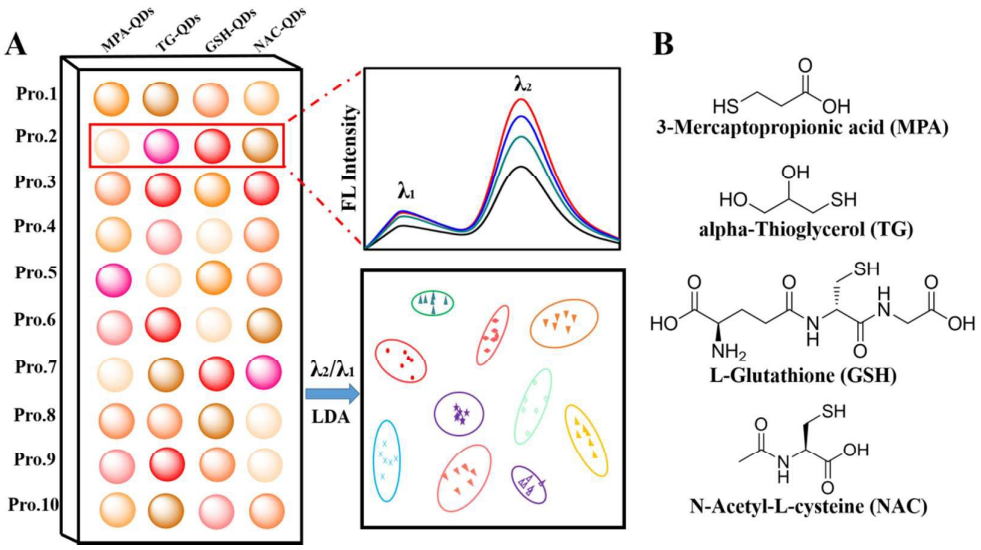

Fig.1 Schematic of the ratiometric fluorescence sensor array based different functionalized QDs for discrimination of proteins; (A) The wells of the microplate contain QDs functionalized by different ligands, and the addition of protein analytes produces a fluorescence pattern; (B) Chemical structures of the different ligands were modified on the surface of QDs. The terminal mercapto group coordinated with QDs, and the other terminal group determined the different features of QDs.

Here we developed a ratometric strategy that used signal ratios of emission intensities at two different peaks instead of two types of signal as multidimensional transduction principles for the discrimination of proteins. The discrimination ability for proteins in both buffer and complicated biological matrix was greatly improved using the ratiometric sensor array based on quantum dots (**Fig. 1**). We synthesized four kinds of Mn-doped ZnS QDs modified with different ligands on their surface as array receptors for pattern recognition. Each QD showed two emission peaks at 420 nm (except for alpha-Thioglycerol capped Mn-ZnS QDs at 500 nm) and 602 nm under a single wavelength excitation. We compared the discrimination ability of the sensor array by utilizing one emission signal ($I_{602\ nm}$), two emission signals ($I_{420\ nm}$ and $I_{602\ nm}$) and signal ratios ($I_{602\ nm}$ / $I_{420\ nm}$, except for alpha-Thioglycerol capped Mn-ZnS QDs as $I_{602\ nm}$ / $I_{500\ nm}$), respectively. We found that the variation of optical signal ratios could be used as a fingerprint to accurately discriminate various proteins. The ratiometric sensor array not only provided an improved performance of the protein discrimination in buffer, but also displayed the strong discrimination ability of protein at different pH values and in the complex biological matrix. In this sensing system, the Mn-doped ZnS QDs with different functionalities served as both the target recognition and ratiometric signal sensing elements, which will bring a new concept for design of the ratiometric sensor array based other nanoparticles. Also our work may give a new direction to enhance the discriminating efficiency of the arrays.

Experimental

Sensing Protein Studies. The MPA-QDs was dissolved in phosphate buffer solution (pH = 7.4, 10 mM) to make 200 μg/mL stock solution. 105 μL of QDs solution (final concentration of 50 μg/mL) was mixed with 42 μL of target proteins stock solution (with final concentrations of 50 nM). After incubation for 30 minutes, the fluorescence intensity values of the mixtures at 420 nm and at 602 nm were recorded on Edinburgh FLS-920 instrument with excitation at 294 nm, respectively. Each protein assay against the sensor array was repeated for six replicates. In the analysis of proteins with NAC-QDs, GSH-QDs, and TG-QDs, all other conditions are equivalent to the above test except for the different excitation at 306 nm, 304, and 274 nm, respectively. For the test effect of environmental changes in buffer for sensing proteins, the procedure is the same as the above measure except for different pH values (5.7, 7.4, and 8.3).

Morning urine from a health volunteer was collected and centrifuged for 15 minutes (12,000 rpm) to remove the insoluble matrix. The raw urine was not further treated. In the analysis with human urine samples, each protein was diluted with human urine. All other conditions were equivalent to the above procedure except that buffer solution was replaced with urine. Thus, the eight target proteins with six replicates were tested against our sensor array based on the four kinds of QD to generate (eight proteins × four QDs × six replicates) training data matrix.

Data Processing for Pattern Recognition.[11] The raw data matrix was subject to linear discriminate analysis (LDA) in SYSTAT V13.0.[11b] The raw fluorescence response patterns were transformed to canonical patterns in which the ratio of between-class variance to within-class variance was maximized according to the preassigned grouping. LDA can be used to differentiate quantitatively the response patterns of target proteins. In a blind experiment, the rates of fluorescence patterns of new cases were first converted to canonical scores using discriminate functions established on training samples. The Mahalanobis distance, which is the distance of a case to the centroid of a group in a multidimensional space, was calculated for each new case with respect to the centroid of the various groups (ten proteins) of training samples. The new case

was assigned to the group with shortest Mahalanobis distance. This processing protocol was performed using the SPSS V16.0 program, allowing the assignment of proteins to specific groups.

Results and discussion

The Design of Sensing Elements. Initially, to investigate the feasibility of these four types of QDs for the discrimination, each protein with the concentration of 150 nM was mixed with MPA-QDs (50 μg/mL). After incubation at room temperature for half an hour, their fluorescent emissions were record from 360 to 750 nm with at excitation 294 nm (**Fig. S2A, ESI**†). The QDs showed a stronger emission at 602 nm and a weaker emission at 420 nm using a single-wavelength excitation, which are ascribe to the emission from Mn-doped ions and host ZnS QDs, respectively. In the sensing studies, the intensities of QDs at 602 nm in PBS buffer (10 mM, pH 7.4) were measured before and after addition of protein analytes. The signal change value was defined as I/I_0, where I and I_0 were the photoluminescence intensity of QDs solution in the presence and absence of the target proteins, respectively. The fluorescent response of ten proteins using MPA-QDs were obtained in **Fig. 2A**. It was observed that the fluorescent intensity of mixture displayed different change compared to blank QDs. For example, HSA enhanced the fluorescence of MPA-QDs and its corresponding value of I/I_0 was 1.11 in **Fig. 2A**. The previous literature demonstrated that HSA could increase the fluorescence of CdTe QDs because of the diminishing of surface defects.[12] Yan's group reported that the fluorescent decay time of MPA-QDs increased somewhat in the presence of HSA. They speculated that the interactions of HSA with MPA-QDs also resulted in a decrease of surface defects, thereby enhancing the fluorescent intensity. Some proteins, such as Cyt-c, Myo, HRP, and Hem greatly quenched the fluorescence of QDs, and these I/I_0 values were 0.60, 0.83, 0.83, and 0.61, respectively. All four metalloproteins contain the Fe heme, which is an effective electron-transfer quencher for CdSe@ZnS QDs.[13] Yan's group also found that the fluorescent lifetime of MPA-QDs was greatly shortened in addition of these proteins,[9] thus the quenching mechanism became possible through electron transfer and the quenching differences depended on the structure diversity of these proteins.[14] On the other hand, these I/I_0 values using MPA-QD, TG-QDs, GSH-QDs and NAC-QDs for sensing HSA were 1.11, 1.06, 0.92, and 1.02, respectively. The fluorescent intensities of all kinds of QDs were enhanced except for GSH-QDs in **Fig. 2B**. The different charged ligands can be designed to tune the electrostatic interactions between QDs and the target proteins, which generated the distinct fluorescent response. These chemical groups including hydroxy, formamide, and carboxyl enable supramolecular interactions with target proteins through hydrogen-bonding, Vander Waals forces, and electrostatic forces. Remarkably, MPA-QDs could be created as a differential receptor, which is not high selective and specific response for a particular protein, while is broad cross-reactive response for many proteins. At the same time, these as-prepared four kinds of QDs exhibited differential fluorescent response for the same protein HSA. In addition, the similar optical properties of the four kinds of QDs make them suitable for array-based pattern recognition (**Fig. S3, ESI**†). These results demonstrated that the fluorescent sensor array based on QDs decorated by different functional groups could be designed for the recognition of target proteins.

Ratimetric Fluorescent Sensor Array Based on QDs for Protein Recognition. We test the ability of our sensor array based on the four kinds of QDs (50 μg/mL) to distinguish different proteins (50 nM) in phosphate buffer (pH 7.4, 10 mM). The fluorescent response pattern at emission peak 602 nm was quantitatively analyzed using LDA. Six replicates were tested for each protein. The raw data was processed to LDA to obtain four canonical factors (94.3, 3.4, 1.7, and 0.6% of the variation), which represent linear combinations of the fluorescence response matrix (four QDs × ten proteins × six replicates). The first two most significant discrimination factors were used to generate a 2D plot (**Fig. 3A**), in which each point represents the response pattern for an individual protein sample against the sensor array. Importantly, we were able to classify the 60 canonical fluorescence response patterns (ten proteins × six replicates) into ten distinct groups. One half of the protein targets were clearly differentiated in this pattern recognition using the fluorescent response of a single emission peak. However, HRP and IgG were not separated from each other. Three proteins (HSA, BSA, and Try) exhibited significant overlap, and one protein (BSA) were not able to obviously separate each other between their 95% confidence ellipses. These results suggested that discrimination ability of proteins using this array with a single emission is limited.

Clearly, the creation of receptors with multimode transduction

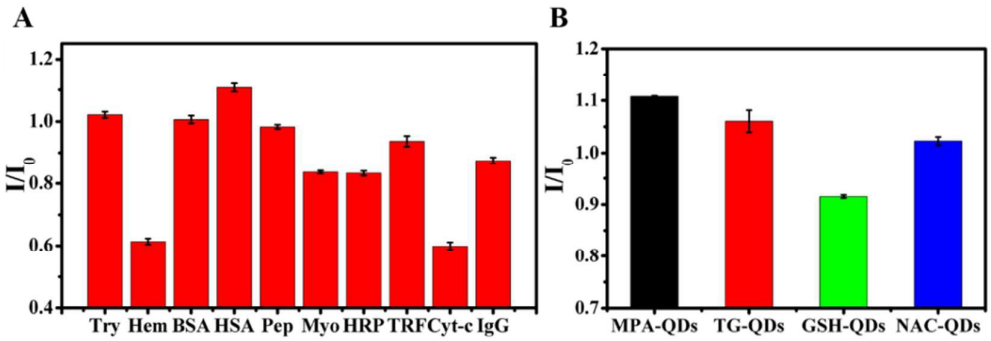

Fig. 2 (A) The fluorescence response of the different proteins to MPA-QDs solution; (B) The fluorescence response of HSA to four kinds of QDs solution. The concentration of each protein is at 150 nM. The fluorescent intensity was obtained at emission 602 nm. Bar height and the error bar represents average of six replicates and the standard deviation, respectively.

principles is one of the most important methods to improve the resolving power of a sensor array.[15] These four kinds of QDs offered unique and well-resolved dual emission bands at ~602 nm of red emission and ~420 nm (~500 nm for TG-QDs) of blue emission under a single wavelength excitation, respectively (**Fig. S2, ESI†**). To enhance the discrimination ability of proteins in this array, we chose two peaks for fluorescent emission data acquisition for further analysis. The distinct response pattern of proteins against our dual-channel sensor array based on these QDs was achieved, and thus 480 data points (dual channels × four QDs × ten proteins × six replicates) were produced for this array. A set of 8-dimensional (four sensors × two wavelengths) data from each protein was obtained, which largely increased the abundance of information about the samples. The raw data was subjected to LDA. The first two most important factors was employed to generate a 2D canonical score plot (**Fig. 3B**). Remarkably, the dual-channel sensor array was employed, so nine out of ten were clearly separated from those of other proteins. As shown in **Fig. 3B**, it can be observed that the dual-channel sensor array appear to have higher discrimination ability compared to a single channel sensor array. Despite the increased the classification accuracy, Pep and BSA still showed significant overlap in the 2D canonical score plot.

We further presented the ratiometric fluorescent sensor array was used to sensing proteins. In the sensing studies, the intensities of the fluorescence (FL) signals of the four types of QDs solution were recorded before and after addition of protein analytes. The ratiometric signal change value was defined as k/k_0, where k and k_0 are the FL intensity ($k = I_{602\ nm} / I_{420\ nm}$) of the QDs solution except for TG-QDs ($k = I_{602\ nm} / I_{500\ nm}$) in the presence and absence of the target proteins, respectively. The responses were compiled into a training matrix, and distinct combinations of fluorescent responses were observed for each analyte protein (**Fig. S7, ESI†**). The raw data were processed using LDA to generate four canonical factors (73.6, 25.7, 0.6, and 0.1% of the variation). The first two discrimination factors were employed to generate a two dimensional 2D plot (**Fig. 3C**). All 60 cases (ten proteins × six replicates) were easily clustered into ten distinct protein groups. The classification accuracy was increased from 98% for dual-channel array to 100% for ratiometric ones according to the jackknifed classification matrix. Compared to the ratiometric fluorescence sensor array, dual-channel method offered poorer resolving power of proteins. Because the response signal changes of these two emission peaks from the optical characteristic could not be completely orthogonal or complementary. This clear discrimination demonstrated that the ratiometric sensor array can accurately detect and identify proteins. Due to the low classification accuracy, the training matrix from a single emission and dual-channel fluorescence response was unsuitable for unknown identification. To test the reproducibility of the ratiometric sensor array, another 30 protein samples were prepared randomly and used as unknowns in a blind experiment. The new cases were classified to the groups generated through the training matrix according to their Mahalanobis distances using LDA analysis. Of 30 cases, 30 were correctly classified, affording an identification accuracy of 100% (**Table S12, ESI†**). This result confirms the reproducibility of our fluorescence patterns.

Effect of Assay Solution pH Value on Sensing Proteins. The inherent superiority of ratiometric sensing strategy is that it can offer more reliable signals. Generally, the traditional sensors that are only dependent on the fluorescent intensity of a single emission wavelength are susceptible to errors caused by some changes in sensor concentration, sample environmental pH value, instrumental artifact, etc.[16] The ratiometric strategy can eliminate these errors because the intensity ratio of two wavelengths is taken. To test the self-referencing capability, we then studied effects of pH value on the protein recognition against the sensor array based on QDs. As illustrated in **Fig. 4A**, **B**, and **C**, it was observed that ten proteins were clearly separated from each other in PBS buffer at pH 5.7 and 7.4. While these samples appeared slight overlap at pH 8.3 in 2D plot. Nonetheless, a three-dimensional LDA score plot (**Fig. S4, ESI†**) shows very good clustering of 240 experimental trials on the 10 proteins. These results indicated that this ratiometric fluorescence sensor array is suitable for further application under physiological conditions. As shown in **Fig. 4D**, **E**, and **F**, one half of these proteins were hardly identified in this pattern recognition using a single emission intensity change of fluorescent response pattern at different pH (5.7, 7.4, and 8.3). These all canonical plots were

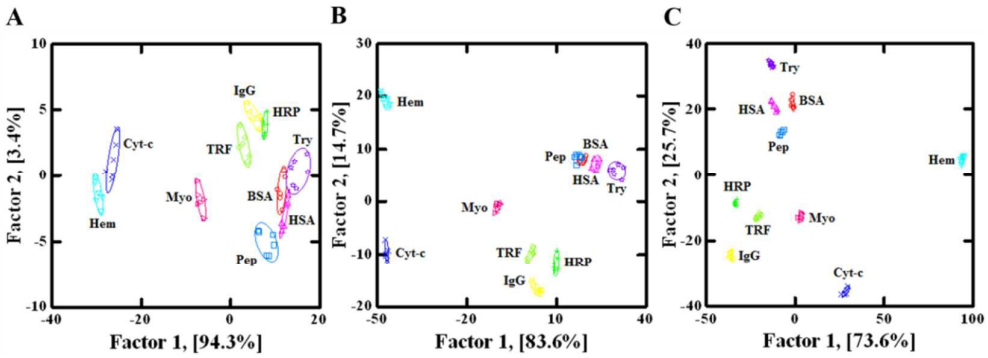

Fig. 3 Sensing of proteins at 50 nM concentration; (A) Canonical score plot for fluorescence response of a single emission against the QDs-based sensor array showing significantly overlapping clusters as compared to the ratiometric fluorescence response; (B) Canonical score plot for the dual-channel fluorescence response also exhibiting slightly compressed groups as compared to the ratiometric fluorescence pattern; (C) Canonical score plot for the ratiometric sensor array. Bar height and the error bar represents average of six replicates and the standard deviation, respectively.

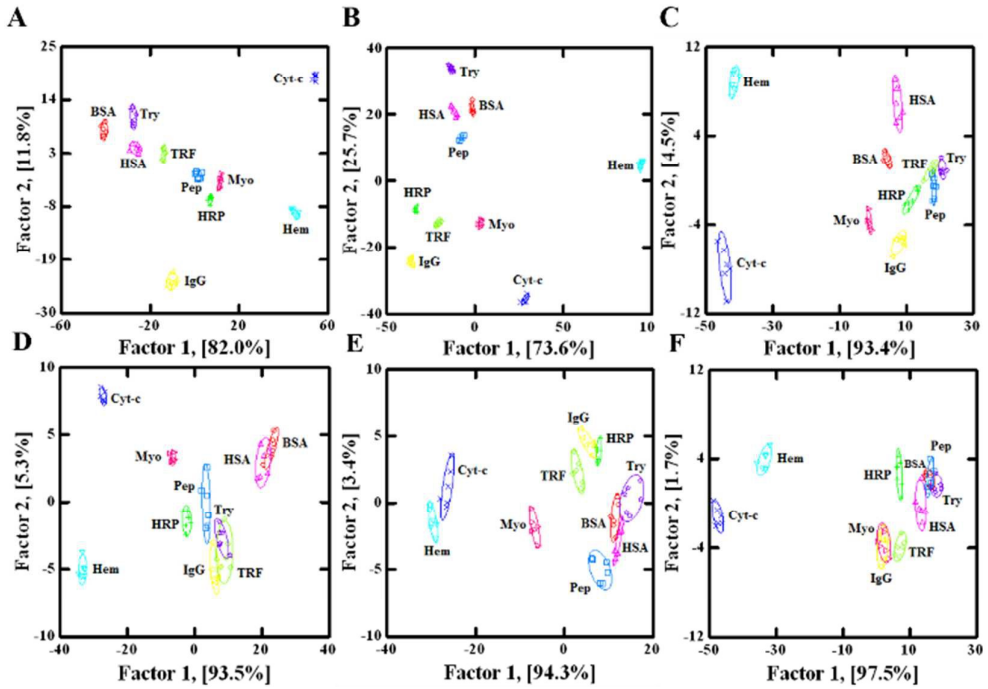

Fig. 4 pH effect on sensing of proteins at 50 nM concentration; (A), (B), (C) Canonical score plot for the ratiometric sensor array at pH 5.7, 7.4, 8.3, respectively; (D), (E), (F) Canonical score plot for the single emission sensor array at pH 5.7, 7.4, 8.3, respectively.

significantly compressed and overlapped. The extremely high dispersion of our ratiometric sensor array data reflects the resistance of interference of outside environment using four sensor elements with the ratios of two emissions peaks. Consequently, different structure and physicochemical proteins are easily recognizable, and even closely structure proteins (BSA and HSA) can be distinguished. In contrast, these two proteins cannot be differentiated using the fluorescent signal recording technologies of a single emission. The jackknifed classification matrix gave the classification accuracy with 100% at different pH using the ratiometric array. Comparably, it showed that the accuracy at pH 5.7, 7.4, and 8.3 was 93%, 98%, and 93% in fluorescent response pattern of a single emission, respectively. The reproducibility of our ratiometric QDs-based sensor array was validated at different pH solutions by testing the unknown samples randomly taken from the training set at the 50 nM. The identification accuracy of the unknown samples was 96.7%, 100%, and 96.7% at pH 5.7, 7.4, and 8.3, respectively (**Table S11, S12, and S13, ESI**†). This clear discrimination meant that the ratiometric strategy can eliminate effect of different pH on sensing proteins.

Analysis of Proteins Spiked in Human Urine. The applicability of our ratiometric sensor array was further investigated for the identification of proteins in the presence of human urine. Sensing proteins is more required in real-world biofluids such as proteins in human urine than a simple buffer solution. Because human urine features more than 1500 proteins and the overall content is more than 1.5 μM (150 mg/L),[17] which greatly compete with the various biomolecules. Moreover, human urine contains high optical background. The complex matrix of human urine is the challenging for sensor array design. The higher concentrations of proteins (500 nM) were detected to obtain adequate signal-to-noise ratios for recording reproducible clusters, while the concentrations of four kinds of QDs at 50 μg/mL remain the same as the experiment described above. As shown in **Fig. 5A**, the majority of the target proteins was not distinguished from those another using fluorescent intensity of a single emission, possibly arising from the complex matrix nature of human urine. However, the eight proteins in the presence of human urine were still completely distinguished employing the ratiometric fluorescence system (**Fig. 5B**). These results indicated that the capability of the ratiometric sensor array for discriminating proteins was not affected by the presence of complex matrix of human urine sample in QDs solution. The reproducibility of our ratiometric QDs-based sensor array was validated by testing the unknown samples randomly taken from the training set. The identification accuracy of the unknown samples was 95.83% (23 out of 24) at the 500 nM (**Table S14, ESI**†).

Conclusions

In summary, we have developed the ratiometric fluorescent sensor array for highly sensitive discrimination of proteins based on Mn-doped ZnS QDs. The rational design of four kinds of QDs decorated different functional group as array receptors offered unique and well-resolved dual emission bands under a single wavelength excitation. Ten proteins at 50 nM were successfully discriminated using the ratiometric sensor array, and the identification accuracy of the unknown samples was 100% (at pH 7.4). This sensor system could eliminate effectively the signal interference from the changes of broad pH range 5.7-8.3 by the analysis of two emission intensity ratio. Furthermore, the protein

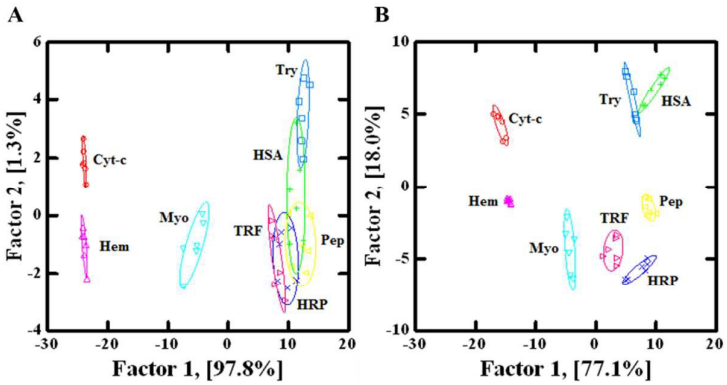

Fig. 5 Discriminant analysis of the QDs sensors responses to eight proteins at 500 nM in the human urine. Results of four kinds of QDs responses for each protein projected on the first two discrimination factors. Ellipses indicate 95 % confidence level; (A) A single emission (at 602 nm); (B) The ratio of two emission peaks ($k = I_{602\,nm} / I_{420\,nm}$, except for TG-QDs $k = I_{602\,nm} / I_{500\,nm}$). The concentration of QDs is at 50 μg/mL.

discrimination ability of this system was not sacrificed even in real biological matrix. This strategy exploits the tunability of the QD nanoparticles surface to provide selective interactions with analytes, and the different fluorescence response of the assembled nanoparticles to impart efficient transduction of the binding event. The present study will broaden the application field of QD-based fluorescence sensors and give new direction to enhance the discriminating efficiency of the arrays.

Acknowledgements

We acknowledge the National Natural Foundation of China (Grant No. 21105066, No. 21405090, No. 21125525) and the Ministry of Science and Technology of China (No. 2012YQ12006003)

Notes and References

1 (a) Rana, S.; LeNgoc, D. B.; Mout, R.; Saha, K.; Tonga, G. Y.; BainRobert, E. S.; Miranda, O. R.; Rotello, C. M.; Rotello, V. M., Nat. Nanotechnol. 2014, 10, 65-69; (b) Li, X.; Kong, H.; Mout, R.; Saha, K.; Moyano, D. F.; Robinson, S. M.; Rana, S.; Zhang, X.; Riley, M. A.; Rotello, V. M., ACS Nano 2014, 8, 12014-12019; (c) Bajaj, A.; Miranda, O. R.; Kim, I.-B.; Phillips, R. L.; Jerry, D. J.; Bunz, U. H. F.; Rotello, V. M., Proc. Natl Acad. Sci. 2009, 106, 10912-10916; (d) You, C. C.; Miranda, O. R.; Gider, B.; Ghosh, P. S.; Kim, I. B.; Erdogan, B.; Krovi, S. A.; Bunz, U. H. F.; Rotello, V. M., Nat. Nanotechnol. 2007, 2, 318-323; (e) Rakow, N. A.; Suslick, K. S., Nature 2000, 406, 710-713; (f) Motiei, L.; Pode, Z.; Koganitsky, A.; Margulies, D., Angew. Chem. Int. Ed. 2014, 53, 9289-9293.

2 (a) Medintz, I. L.; Uyeda, H. T.; Goldman, E. R.; Mattoussi, H., Nat. Mater. 2005, 4, 435-446; (b) Wu, P.; Yan, X.-P., Chem. Soc. Rev. 2013, 42, 5489-5521; (c) Chan, W. C. W.; Nie, S., Science 1998, 281, 2016-2018; (d) Bruchez, M.; Moronne, M.; Gin, P.; Weiss, S.; Alivisatos, A. P., Science 1998, 281, 2013-2016; (e) Han, M.; Gao, X.; Su, J. Z.; Nie, S., Nat. Biotech. 2001, 19, 631-635; (f) Murphy, C. J., Anal. Chem. 2002, 74, 520 A-526 A.

3 Liu, Q.; Yeh, Y.-C.; Rana, S.; Jiang, Y.; Guo, L.; Rotello, V. M., Cancer Lett. 2013, 334, 196-201.

4 Liu, J.; Li, G.; Yang, X.; Wang, K.; Li, L.; Liu, W.; Shi, X.; Guo, Y., Anal. Chem. 2015, 87, 876-883.

5 (a) Erwin, S. C.; Zu, L.; Haftel, M. I.; Efros, A. L.; Kennedy, T. A.; Norris, D. J., Nature 2005, 436, 91-94; (b) Norris, D. J.; Efros, A. L.; Erwin, S. C., Science 2008, 319, 1776-1779.

6 (a) Yang, H.; Santra, S.; Holloway, P. H., J. Nanosci. Nanotechnol. 2005, 5, 1364-1375; (b) Thakar, R.; Chen, Y.; Snee, P. T., Nano Lett. 2007, 7, 3429-3432; (c) He, Y.; Wang, H.-F.; Yan, X.-P., Anal. Chem. 2008, 80, 3832-3837; (d) Zou, W.-S.; Sheng, D.; Ge, X.; Qiao, J.-Q.; Lian, H.-Z., Anal. Chem. 2011, 83, 30-37.

7 Wu, P.; Zhao, T.; Tian, Y.; Wu, L.; Hou, X., Chem. Eur. J. 2013, 19, 7473-7479.

8 Sang, L.-J.; Wang, H.-F., Anal. Chem. 2014, 86, 5706-5712.

9 Wu, P.; Miao, L.-N.; Wang, H.-F.; Shao, X.-G.; Yan, X.-P., Angew. Chem. Int. Ed. 2011, 50, 8118-8121.

10 Hierlemann, A.; Gutierrez-Osuna, R., Chem. Rev. 2008, 108, 563-613.

11 (a) Bajaj, A.; Miranda, O. R.; Phillips, R.; Kim, I.-B.; Jerry, D. J.; Bunz, U. H. F.; Rotello, V. M., J. Am. Chem. Soc. 2010, 132, 1018-1022; (b) Jurs, P. C.; Bakken, G. A.; McClelland, H. E., Chem. Rev. 2000, 100, 2649-2678.

12 (a) Wang, J.-H.; Wang, H.-Q.; Zhang, H.-L.; Li, X.-Q.; Hua, X.-F.; Huang, Z.-L.; Zhao, Y.-D., Colloids Surf. A 2007, 305, 48-53; (b) Gerhards, C.; Schulz-Drost, C.; Sgobba, V.; Guldi, D. M., J. Phys. Chem. B 2008, 112, 14482-14491.

13 Sharon, E.; Freeman, R.; Willner, I., Anal. Chem. 2010, 82, 7073-7077.

14 Ma, Y.; Bai, H.; Yang, C.; Yang, X., Analyst 2005, 130, 283-285.

15 Mitrovics, J.; Ulmer, H.; Weimar, U.; Göpel, W., Acc. Chem. Res. 1998, 31, 307-315.

16 Tyrakowski, C. M.; Snee, P. T., Anal. Chem. 2014, 86, 2380-2386.

17 (a) Adachi, J.; Kumar, C.; Zhang, Y.; Olsen, J. V.; Mann, M., Genome Biol. 2006, 7, R80-R80; (b) Fliser, D.; Novak, J.; Thongboonkerd, V.; Argiles, A.; Jankowski, V.; Girolami, M. A.; Jankowski, J.; Mischak, H., J. Am. Soc. Nephrol. 2007, 18, 1057-1071; (c) Li, S. J.; Peng, M.; Li, H.; Liu, B. S.; Wang, C.; Wu, J. R.; Li, Y. X.; Zeng, R., Nucleic Acids Res. 2009, 37, D907-D912.